

The structure and structural pressure dependence of sodium deuterioxide-V by neutron powder diffraction

This article has been downloaded from IOPscience. Please scroll down to see the full text article.

1996 J. Phys.: Condens. Matter 8 L597

(<http://iopscience.iop.org/0953-8984/8/41/001>)

View [the table of contents for this issue](#), or go to the [journal homepage](#) for more

Download details:

IP Address: 171.66.16.207

The article was downloaded on 14/05/2010 at 04:16

Please note that [terms and conditions apply](#).

LETTER TO THE EDITOR

The structure and structural pressure dependence of sodium deuterioxide-V by neutron powder diffraction

J S Loveday[†], W G Marshall[†], R J Nelmes[†], S Klotz^{‡§}, G Hamel^{||} and J M Besson[‡]

[†] Department of Physics and Astronomy, The University of Edinburgh, Edinburgh EH9 3JZ, UK

[‡] Physique des Milieux Condensés (CNRS URA 782), Université Pierre et Marie Curie, B77, 4 Place Jussieu 75252 Paris, France

^{||} Département des Hautes Pressions, Université Pierre et Marie Curie, B77, 4 Place Jussieu 75252 Paris, France

[§] Laboratoire Léon Brillouin, CEN Saclay, F91191, Gif-sur-Yvette, France

Received 9 August 1996

Abstract. The full structure of the high-pressure phase V of sodium deuterioxide has been solved from neutron powder diffraction data and its structural pressure dependence has been measured up to 8.6 GPa. The structure reveals that NaOD-V is hydrogen bonded, but with bent and possibly bifurcated hydrogen bonds. With increasing pressure, one of the deuterium oxygen contacts shortens more rapidly than the other and this hydrogen bond straightens.

There has been a long-standing interest in the behaviour of hydrogen-bonded materials at high pressure aimed at exploring the changes in interatomic potentials with density. Such information is important to the understanding of a wide range of problems from the high-pressure behaviour of ice and other hydrides of non-metallic elements [1–3] to the properties of hydrated minerals at pressures found in the mantle [4].

The alkali hydroxides are an important and interesting group of materials. They are arguably the simplest non-molecular hydrogen-bonded compounds and, as a group, have similar structural systematics [5–9]. A feature of this group is that while the heavy-alkali hydroxides KOH(D), RbOH(D) and CsOH(D) exhibit hydrogen bonding, the lightest member LiOH(D) does not [6, 10]. Sodium hydroxide is of particular interest as it appears to be close to the boundary between hydrogen bonded and non-hydrogen bonded structures. The only one of its phases *known* to exhibit hydrogen bonding is phase IV[¶] which is stable at low temperatures and is found at ambient pressure only in the deuterated form [7]. Under pressure, its behaviour appears to be anomalous. Both NaOH and NaOD form a layered structure at ambient pressure and temperature with a square-like array of Na–O units arranged head to tail within each layer; the O–H bonds are directed into the space between the layers [11]. This structure transforms to phase V at ~ 1 GPa at room temperature and ~ 5 GPa at 70 K [12]. X-ray studies showed that this phase is orthorhombic and found a non-layered distorted NiAs structure for the heavy atoms, with spacegroup *Pbcm* or *Pbc2₁* [13]. The changes in vibrational frequencies with pressure have been explored by Raman and infra-red studies [12]. These show softening of the O–H vibron with pressure in

[¶] There are several numbering schemes for the phases of sodium hydroxide in the literature. We have chosen to adopt that used in the papers from the Paderborn group [12, 5]. Thus the high-temperature fcc and monoclinic forms are phases I and II respectively, the ambient-pressure and temperature phase is phase III, the low-temperature ambient-pressure phase of NaOD is phase IV and the high-pressure phase discussed here is phase V.

phase IV—the hydrogen-bonded low-temperature phase—but the transformation to phase V is accompanied by a stepwise *increase* in the frequency back almost to the ambient-pressure value, and within phase V the vibron frequency shows almost no change with pressure. This is highly unexpected; as has been stated, vibron softening is considered to be a good indicator of increasing hydrogen-bond strength, and pressure is generally found to produce vibron softening in hydrogen-bonded materials—as is found in potassium, rubidium and caesium hydroxides [10]. The absence of softening of the vibron in sodium hydroxide phase V led Krobok *et al* [12] to conclude that linear hydrogen bonds with O–H...O angles close to 180° were absent and that hydrogen bonds in this phase were either bifurcated, bent or absent. On the basis of an examination of cation movements at the III → V transition, Beck and Lederer [13] proposed an arrangement where the O–H bonds are directed towards neighbouring sodium atoms, an arrangement which appears to have no hydrogen bonds.

It is clearly interesting to establish directly the location of the hydrogen atoms in sodium hydroxide-V and hence their bonding geometry. Highly bent or bifurcated hydrogen bonds are rare at ambient pressure [14]. However they are emerging as a more common feature of high-pressure structures—for example, they have been found in a number of important water-containing minerals [15] and in the high-pressure phase IV of ammonia [16]. That such hydrogen bonds have been suggested to exist in a material as simple as sodium hydroxide is somewhat remarkable. However, neither x-ray nor Raman studies have been able to conclusively settle the nature of the bonding of hydrogen atoms. We now present a full solution of the structure of NaOD-V from neutron diffraction data and measurements of the structural pressure dependence.

Neutron diffraction data were collected using the Paris–Edinburgh opposed-anvil cell. This cell [17] is designed to achieve pressures of up to 10 GPa with a sample volume of ~100 mm³ or 25 GPa with a sample volume of 25 mm³—volumes which are sufficiently large for accurate structural studies using neutron diffraction. This development, which represents a tenfold increase in the pressure range for neutron diffraction [18], makes it possible for the first time to determine the precise location of hydrogen atoms over a sufficient pressure range to produce measurable changes in bond geometry.

Samples of NaOD were prepared by dehydration of a solution of 40 wt% NaOD in D₂O solution—purchased from the Aldrich Chemical Company—in a vacuum oven at 250 °C. The resulting powder was pressed under argon atmosphere into a pellet and loaded between the opposed (tungsten carbide) anvils of the pressure cell along with fluorinert hydrostatic fluid, and surrounded by a Ti/Zr alloy gasket. Pressure was achieved by the application of load to the anvils by an *in situ* hydraulic ram, as described in [17].

Time-of-flight neutron diffraction data were collected at the UK pulsed neutron facility, ISIS, at the Rutherford Appleton Laboratory, during the commissioning of a new facility specifically designed for high-pressure experiments using the Paris–Edinburgh cell and installed on the first sample position of a recently upgraded high-pressure and engineering beamline, PEARL, on a 177 K methane moderator. The new installation is particularly well suited to the solution of unknown structures at high pressure, for a number of reasons. The high flux of long-wavelength neutrons resulting from the use of the cold methane moderator gives good counting statistics for the long *d*-spacing reflections needed to identify the correct unit cell and spacegroup. In addition, the cell can be mounted in two orientations to access two different banks of detectors and thereby obtain further useful information. The conventional orientation with the incident beam parallel to the cell axis allows detectors placed at $2\theta = 90^\circ (\pm 7^\circ)$ to be used, while an orientation with the cell rotated so that the incident beam is in the plane of the gasket allows access to detectors placed in a vertical plane containing the incident beam—the longitudinal detectors. This second orientation

has two advantages for structure solution. Firstly, it permits scattering at angles other than $2\theta = 90^\circ$, in particular at low 2θ , and a detector placed to cover $2\theta = 20\text{--}40^\circ$ is able to measure reflections with d -spacings up to 11 \AA to test unit cell indexing. Secondly, the change in the relative orientations of the scattering vector and the cell axis also provides a means to test models of preferred orientation without any prior assumptions about the structure [18].

Data were collected at applied loads of 20, 35, 50, 60 and 70 tonnes. The pressures were determined from the measured lattice parameters, using the equation of state [5], as 1.2, 2.9, 4.9, 6.4 and 8.6 GPa respectively for the five loads. Data acquisition times varied between 6 and 10 h with ISIS running at a proton current of $\sim 130 \mu\text{A}$. At pressures of 1.2 and 4.9 GPa, patterns were collected in the longitudinal detectors as well as the 90° bank. The patterns collected were normalized for the incident flux profile measured using the scattering from a vanadium sample, and were also corrected for the effects of wavelength-dependent attenuation by the pressure cell materials using a procedure based on the measured attenuation coefficients of the pressure cell materials and calculations of the relevant pathlengths [19].

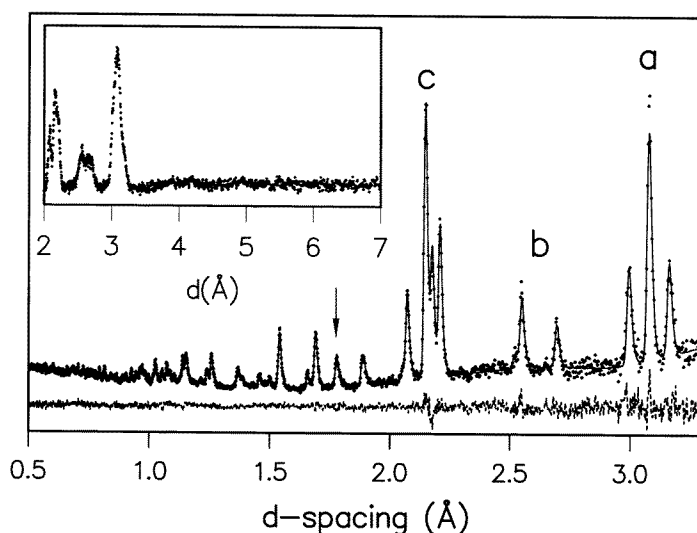


Figure 1. The powder diffraction pattern collected from NaOD-V at 1.2 GPa. The data collected at $2\theta = 90^\circ$ are shown as dots, the solid line is the fit obtained by Rietveld profile refinement as described in the text, and the dashed line is the difference between the observed and calculated profiles. The arrow marks the strongest peak due to scattering from the tungsten carbide anvils. The inset shows the long- d -spacing part of the pattern collected in the low-angle ($2\theta = 20\text{--}40^\circ$) detector bank. The three peaks shown in the inset correspond to the three groups of peaks labelled a, b and c in the main plot. Due to the lower resolution of the low angle detector bank, the peak splittings observed at $2\theta = 90^\circ$ are not visible.

Figure 1 shows the pattern collected at 1.2 GPa. All peaks visible in the main profile are consistent with the unit cell and spacegroup proposed from x-ray data [13] and the known unit cell of tungsten carbide (the anvil material) whose scattering produced some small contaminant peaks (the strongest of these peaks is marked in figure 1), and a pattern collected in the $2\theta = 20\text{--}40^\circ$ bank (see figure 1, inset) showed no extra peaks at long d -spacings. It thus appears that the unit cell and spacegroup derived from the x-ray studies is correct for the full structure. In addition, the relative intensities of the strong reflections

were found not to vary with the change between the conventional and second orientations of the pressure cell, and hence it can be concluded that strong preferred orientation is absent. The pattern shown in figure 1 was used for structure solution using the GSAS suite of programs [20]. The procedure adopted was to place the heavy atoms at the positions determined in the x-ray study [13]—Na on the 4c sites of *Pbcm* at $(0.359, \frac{1}{4}, 0)$ and O on the 4d sites at $(0.800, 0.043, \frac{1}{4})$ —and then refine the D atom positions using the Rietveld method, subject to a soft restraint to keep the O–D bond length close to 0.95 Å. After ~30 cycles of refinement the fit converged sufficiently to allow the restraint to be removed. A good fit to the data was obtained with the structure shown in figure 2, which gives a weighted profile *R* factor of 0.041%.

To verify that this was a unique arrangement, other deuterium arrangements were explored. The deuterium atom was stepped in 10° intervals of two Euler angles over the surface of a sphere of radius ~0.95 Å centred on the oxygen site, and at each position the quality of fit expressed as χ^2 was assessed by profile refinement varying only scale, background and temperature factors. This approach explored two possible types of arrangement: when $z(D) = \frac{1}{4}$ the deuterium atom lies in a mirror plane normal to the *c*-axis (as in figure 2) and the deuterium sites are fully occupied, while when $z \neq \frac{1}{4}$ the arrangement is disordered with half-occupied deuterium sites. The ordered deuterium arrangement corresponding to the fit shown in figure 1 gave a minimum in χ^2 of 1.369, ~6 times lower than any other minimum. This deuterium arrangement is thus clearly unique. The possibility that the true structure has spacegroup *Pbc2₁*—the other spacegroup consistent with the systematic absences—and is actually slightly distorted from that found, was also tested. *Pbc2₁* removes the symmetry restrictions on the *y*- and *z*-co-ordinates of Na and the *z*-co-ordinates of O and D and a model with the atoms close to, but not on, the *Pbcm* special positions was used. Such a model did not give a significant improvement in fit and the refined co-ordinates remained within two estimated standard deviations of the *Pbcm* values. It thus appears that *Pbcm* is the correct spacegroup. For the final refinement, a twelve-term background polynomial and two peak-width parameters (to model the effects of pressure-induced peak broadening) were varied, in addition to the structural parameters listed in table 1. The contaminant scattering from the tungsten carbide anvils was modelled by including tungsten carbide as a second phase in the refinement procedure. The final fit is shown as the solid line in figure 1.

The deuterium and oxygen atoms both lie in layers perpendicular to the *c*-axis at $z = \frac{1}{4}$ and $\frac{3}{4}$ and figure 2 shows the $z = \frac{1}{4}$ layer of the structure viewed along the *c*-axis. The deuterium atoms are arranged such that the O–D bonds lie in this *xy*-plane and are canted at an angle of ~33° to the *a*-axis, giving a two-dimensional O...D network. The O–D distance of 0.957(6) Å is somewhat longer than the value of 0.91(1) Å found in phase III at ambient pressure [11]. However, the deuterium thermal motion in phase III is elongated perpendicular to the O–D bond, indicating either libration or disorder, whereas in NaOD-V at 1.2 GPa the thermal motion is much more isotropic (see table 1). Hence, this apparent change in O–D bondlengths is probably the result of the thermal motion on the apparent O–D bondlength in phase III. The O–D bond is directed towards two oxygen atoms labelled O' and O'' in figure 2 with D...O distances of 2.421(6) and 2.513(6) Å and O–D...O angles of 133.5(6) and 136.2(5)° respectively. The D...O' distance is slightly larger than 2.4 Å, the sum of the van der Waals radii for O and D, which is taken as the usual criterion for a hydrogen bond. However, D...O' is shorter than the value of 2.45 Å in NaOD-IV [7], which *is* hydrogen bonded. It thus appears that at least this contact is a hydrogen bond though the O–D...O' angle deviates a long way from a 180°. This would account for the

Table 1. The refined values of lattice parameters, atomic fractional co-ordinates and thermal parameters of NaOD-V at 1.2 GPa. The sodium atom is located on a 4c ($x, \frac{1}{4}, 0$) site and the oxygen and deuterium atoms on 4d ($x, y, \frac{1}{4}$) sites in spacegroup *Pbcm*.

	Neutron data 1.2 GPa
a (Å)	3.1567(4)
b (Å)	5.9727(7)
c (Å)	6.1420(7)
$x(\text{Na})$	0.3406(16)
$U_{\text{iso}}(\text{Na}) \times 10^2 \text{ \AA}^2$	0.91(14)
$x(\text{O})$	0.7884(12)
$y(\text{O})$	0.0733(6)
$U_{\text{iso}}(\text{O}) \times 10^2 \text{ \AA}^2$	1.16(11)
$x(\text{D})$	0.0403(14)
$y(\text{D})$	0.0158(9)
$U_{11} \times 10^2 \text{ \AA}^2$	3.30(32)
$U_{22} \times 10^2 \text{ \AA}^2$	4.66(32)
$U_{33} \times 10^2 \text{ \AA}^2$	2.70(21)
$U_{12} \times 10^2 \text{ \AA}^2$	-0.35(20)

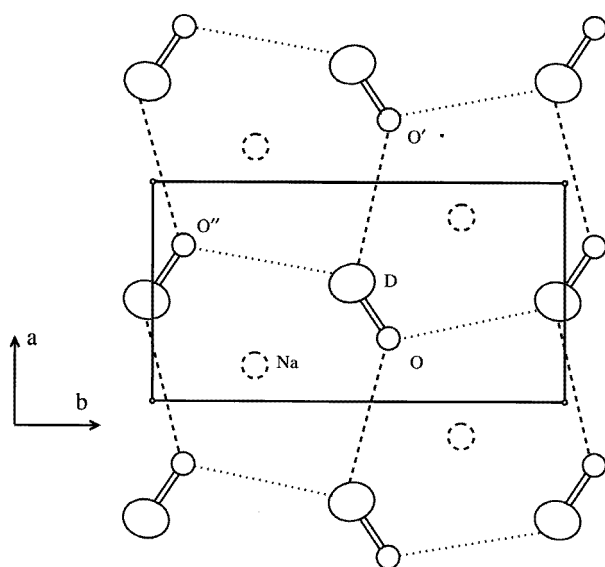


Figure 2. The $z = \frac{1}{4}$ layer of the structure of NaOD-V viewed along the c -axis showing the arrangement of the oxygen and deuterium atoms which lie in this layer. For completeness, the projected positions of the sodium atoms, which lie at $z = 0$ and $z = \frac{1}{2}$, are also shown as dashed circles. The labelled oxygen atoms O, O' and O'' referred to in the text are all equivalent by symmetry. The shorter D...O' contacts are shown as dashed lines and the longer D...O'' contacts as dotted lines.

lack of softening of the O–D vibron with pressure [12]. Whether the D...O'' contact is also a hydrogen bond is less clear. The D...O'' distance is longer than either the standard criterion or the corresponding distance in phase IV and this would suggest that D...O'' is not a hydrogen bond. However, the approximate equivalence of the two O–D...O angles

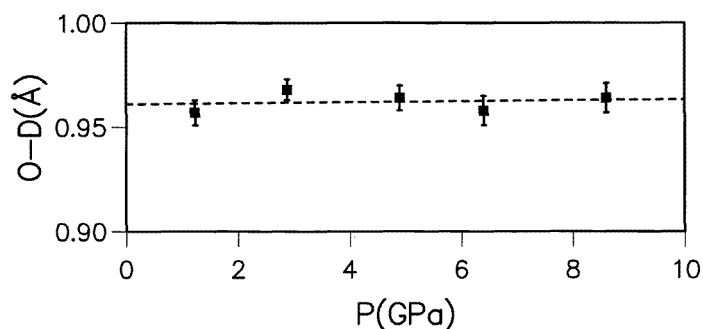


Figure 3. The pressure dependence of the O–D bondlength. The dashed line represents a linear least-squares fit to the values.

would suggest that $D \dots O''$ is also a hydrogen bond contact and that the hydrogen bonds in NaOD are bifurcated. This question is difficult to settle on the basis of information at only one pressure, and so the changes in the structure of phase V with pressure were also explored.

Figure 3 shows the values of the O–D bondlength as a function of pressure along with a linear least-squares fit to the measured values. The fitted rate of change at $2(49) \times 10^{-4} \text{ \AA GPa}^{-1}$ is comparable with the value of $4(4) \times 10^{-4} \text{ \AA GPa}^{-1}$ found in ice-VIII [21] and this is to be expected. Indeed, given that the hydrogen bonding in ice-VIII is stronger than that in NaOD the variation of O–D with pressure in NaOD might be expected to be smaller than that in ice-VIII. However, the precision of the measurements do not allow such a small difference to be detected.

The changes in the hydrogen bond geometry with pressure are shown in figure 4. As can be seen, the shorter contact $D \dots O'$ is compressed more rapidly than $D \dots O''$ and the linear least-squares fits shown yield gradients which differ by a factor of one. The direction of the O–D bond also rotates with increasing pressure such that the O–D $\dots O'$ angle is straightened by $\sim 6^\circ$ while the angle O–D $\dots O''$ becomes more bent by a similar amount. Thus it appears that the $D \dots O'$ contact is strengthened with increasing pressure at the expense of $D \dots O''$. This is in contrast to the behaviour of ammonia phase IV—the only system with a bifurcated hydrogen bond whose structural pressure dependence has been studied to date [16]. In ammonia-IV the longer contact of the bifurcated hydrogen bond appears to increase in strength with increasing pressure. Thus, the measurements of the structural pressure dependence would appear to support the view that the $D \dots O''$ hydrogen bond, if it is indeed a hydrogen bond, is much weaker than $D \dots O'$, and is relatively further weakened by pressure.

Thus, neutron diffraction studies have provided the first direct information on the hydrogen atom positions in NaOD-V and have shown for the first time that this phase is hydrogen bonded with very bent and possibly bifurcated hydrogen bonds. The structural pressure dependence shows large changes in the hydrogen bond geometry which suggest that the longer $D \dots O$ contact is much weaker than the shorter. The ability to follow the structural pressure dependence over a wide range of pressures is important in this study as it permits the relative strengths of the hydrogen bonds to be explored.

We would like to acknowledge the support of a research grant from the Instrument Development Fund of the EPSRC for the construction and development of new high-pressure

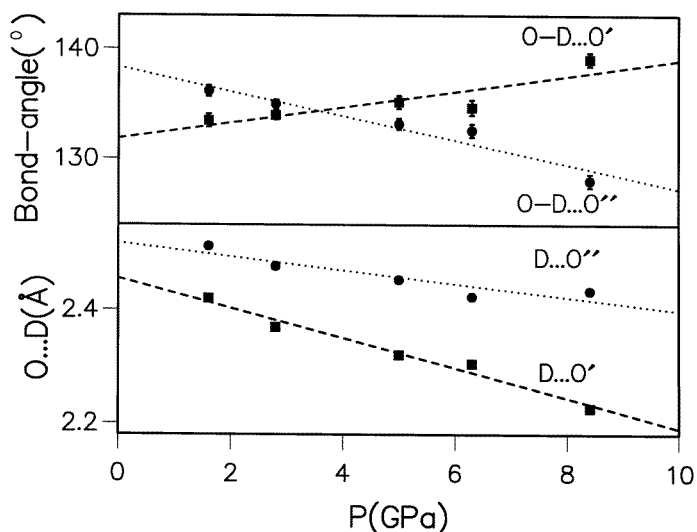


Figure 4. The upper plot shows the variation with pressure of the bond angles of the two O-D...O contacts. The variation of the longer contact angle, O-D...O'', is shown as open circles and that of the shorter, O-D...O', is shown as open squares. The lower plot shows the variation of the corresponding contact lengths D...O'' (filled circles) and D...O' (filled squares). The dotted and dashed lines represent linear least-squares fits to the measured variations.

facilities at ISIs, and thank RAL for the provision of development beamtime and much assistance in the design and installation work on the PEARL beamline. We would also like to acknowledge support from the Institut National des Sciences de l'Univers through the French national programme in Planetary Science, from the French Commissariat à l'Energie Atomique, and from the Commission of the European Community through a fixed contribution contract supporting one of us (SK). Physique des Milieux Condensés is Unité de recherche associée au CNRS no 782.

References

- [1] Holzapfel W B 1972 *J. Chem. Phys.* **56** 712
- [2] Klug D D and Whalley E 1982 *J. Chem. Phys.* **77** 2166
- [3] Pruzan Ph, Chervin J C and Gauthier M 1990 *Europhys. Lett.* **13** 81
- [4] Parise J B, Leinenweber K, Weidner D J, Tan K and Von Dreele R B 1994 *Am. Mineral.* **79** 193
- [5] Otto J W and Holzapfel W B 1995 *J. Phys.: Condens. Matter* **7** 5461-76
- [6] Christy A G, Haynes J and Adams D M 1992 *J. Phys. Chem.* **96** 8173-6
- [7] Bastow T J, Elcombe M M and Howard C J 1986 *Solid State Commun.* **57** 339-41
- [8] Bastow T J, Elcombe M M and Howard C J 1986 *Solid State Commun.* **59** 257-9
- [9] Bastow T J, Elcombe M M and Howard C J 1987 *Solid State Commun.* **62** 149-51
- [10] Krobok M P and Holzapfel W B 1994 *J. Phys.: Condens. Matter* **6** 9789-806
- [11] Bleif H J and Dachs H 1982 *Acta Crystallogr. A* **38** 470-6
- [12] Krobok M P, Johannsen P G and Holzapfel W B 1992 *J. Phys.: Condens. Matter* **4** 8141-50
- [13] Beck H P and Lederer G 1993 *J. Chem. Phys.* **98** 7289-94
- [14] Olovsson I 1976 *Hydrogen Bond* vol 2 (Amsterdam: North-Holland) p 395
- [15] Northrup P A, Leinenweber K and Parise J B 1994 *Am. Mineral.* **79** 404-4
- [16] Loveday J S, Nelmes R J, Marshall W G, Besson J M, Klotz S and Hamel G 1996 *Phys. Rev. Lett.* **76** 74-8
- [17] Besson J M, Nelmes R J, Hamel G, Loveday J S, Weill G and Hull S 1992 *Physica B* **180-1** 907-10

- [18] Nelmes R J, Loveday J S, Wilson R M, Basson J M, Klotz S, Hamel G and Hull S *Trans. Am. Cryst. Ass.* **29** 19–27
- [19] Wright N G, Nelmes R J, Belmonte S A and McMahon M I 1996 *J. Synch. Radiat.* **3** 112–19
- [20] Marshall W G, Nelmes R J, Loveday J S, Besson H M, Klotz S and Hamel G 1995 *Proc. XVIIth IUCr Congr.; Acta Crystallogr.* at press
- Wilson R, Loveday J S, Nelmes R J, Klotz S and Marshall W G 1995 *Nucl. Instrum. Methods A* **354** 145–8
- [21] Larson A C and Von Dreele R B 1986 *Los Alamos National Laboratory Report LAUR 86748*
- [22] Nelmes R J, Loveday J S, Wilson R M, Besson J M, Klotz S and Hamel G 1993 *Phys. Rev. Lett.* **71** 1192–5